

## Measurement report: An assessment of the impact of a nationwide lockdown on air pollution – a remote sensing perspective over India

Mahesh Pathakoti<sup>1\*</sup>, Aarathi Muppalla<sup>2</sup>, Sayan Hazra<sup>3</sup>, Mahalakshmi DV<sup>1</sup>, Kanchana Asuri Lakshmi<sup>1</sup>, Vijay Kumar Sagar<sup>1</sup>, Raja Shekhar<sup>2</sup>, Srinivasulu Jella<sup>1</sup>, Sesha Sai MVR<sup>1</sup>, Uma Vijayasundaram<sup>3</sup>

<sup>1</sup>Earth and Climate Sciences Area (ECSA), National Remote Sensing Centre (NRSC), Indian Space Research Organization (ISRO), Hyderabad-500037, India.

<sup>2</sup>Bhuvan Geoportal and Data Dissemination Area, NRSC, ISRO, Hyderabad-500037, India.

<sup>3</sup>Department of Computer Science, School of Engineering & Technology, Pondicherry University, Chinna Kalapet, Kalapet, Puducherry-605014, India

\*Correspondence to Mahesh P (mahi952@gmail.com)

**Abstract.** The nationwide lockdown was imposed over India from 25<sup>th</sup> March to 31<sup>st</sup> May 2020 with varied relaxations from phase-I to phase-IV to contain the spread of COVID-19. Thus, emissions from industrial and transport sectors were halted during lockdown (LD) which resulted in a significant reduction of anthropogenic pollutants. The first two lockdown phases were strictly followed (phase-I and phase-II) and hence are considered as total lockdown (TLD) in this study. Satellite-based tropospheric columnar nitrogen dioxide (TCN) from the years 2015 to 2020, tropospheric columnar carbon monoxide (TCC) during 2019-2020, and aerosol optical depth (AOD<sub>550</sub>) from the years 2014 to 2020 during phase-I and phase-II LD and pre-LD periods were investigated with observations from Aura/OMI, Sentinel-5P/TROPOMI, and Aqua-Terra/ MODIS. To quantify lockdown-induced changes in TCN, TCC, and AOD<sub>550</sub>, detailed statistical analysis was performed on de-trended data using the student's paired statistical t-test. Results indicate that mean TCN levels over India showed a dip of 18% compared to the previous year and also against the 5-year mean TCN levels during the phase-I lockdown, which was found statistically significant (p-value <0.05) against the respective period. Furthermore, drastic changes in TCN levels were observed over hotspots namely the eastern region and urban cities. For example, there was a sharp decrease of 62% and 54% in TCN levels as compared to 2019 and against 5-year mean TCN levels over New Delhi with a p-value of 0.0002 (which is statistically significant) during total LD. The TCC levels were high in the North East (NE) region during the phase-I LD period, which is mainly attributed to the active fire counts in this region. However, lower TCC levels are observed in the same region due to the diminished fire counts during phase-II. Further, AOD<sub>550</sub> is reduced over the country by ~16 % (Aqua and Terra) from the 6-year (2014-2019) mean AOD<sub>550</sub> levels, with a significant reduction (Aqua/MODIS 28%) observed over the Indo-Gangetic plains (IGP) region with a p-value of <<0.05. However, an increase in AOD<sub>550</sub> levels (25% for Terra/MODIS, 15% for Aqua/MODIS) was also observed over Central India during LD compared to the preceding year and found

35 significant with a p-value of 0.03. This study also reports the rate of change of TCN levels and AOD<sub>550</sub> along with statistical metrics during the LD period.

**Keywords:** COVID-19, lockdown, Satellite, TCN, TCC, AOD<sub>550</sub>

## 1. Introduction

40 Following the outbreak of the novel coronavirus disease (COVID-19) and its declaration as a pandemic by the World Health Organization (WHO) on 11<sup>th</sup> March 2020, several countries across the globe imposed national lockdowns to contain the pandemic (e.g., Tian et al., 2020). India confirmed its first COVID-19 case on 30<sup>th</sup> January 2020 with an exponential increase to 360 cases by 22<sup>nd</sup> March 2020 (<https://www.mohfw.gov.in/>). In an attempt to restrict this pandemic, the Indian government called for a ‘Janata Curfew’ on 22<sup>nd</sup> March 2020, followed 45 by nationwide lockdown (LD) in a phased manner starting from 25<sup>th</sup> March – 14<sup>th</sup> April 2020 (21 days) as phase-I, 15<sup>th</sup> April – 3<sup>rd</sup> May 2020 (19 days) as phase-II, 4<sup>th</sup> May – 17<sup>th</sup> May 2020 (14 days) as phase-III and 18<sup>th</sup> May – 31<sup>st</sup> May in 2020 (14 days) as phase-IV. Under this lockdown, 1.30 billion citizens of India were advised to stay indoors, all the domestic and international flights, transport, and industrial production were suspended, and only essential services were permitted. However, agriculture farming and its related sectors are permitted during phase-50 II as India is an agricultural-dependent country. As indicated above, indoor emissions (cooking) and emissions from the emergency services were still present in phase-I. For phase-II, crop residue burnings were added in addition to phase-I emissions. Except for these, the rest of the anthropogenic emissions from the above sectors are completely shut during phase-I and phase-II. Thus, economic activities were greatly affected and hence there was a shortfall in net energy consumption by about 30% (<https://www.ppac.gov.in/>) during the strict lockdown period 55 (first two lockdown phases).

Air pollution has arisen as an environmental issue that is harmful to human health (Xu et al., 2020) and extends from local to global scale (Fang et al., 2009). The oxides of nitrogen (NO, NO<sub>2</sub>) play important role in tropospheric chemistry and climate change. Exposure to nitrogen dioxide (NO<sub>2</sub>) has been correlated with an increased rate of morbidity and subsequently increased rate of mortality (WHO, 2013). Global emissions of NO<sub>x</sub> 60 (NO, NO<sub>2</sub>) are primarily due to anthropogenic activities such as transportation (32% in India), industrial activities (21% in India), thermal power plants (28% in India), biomass burning (19% in India) whereas the natural sources of NO<sub>x</sub> are soils and lightning (Biswal et al., 2021). Thus, the hotspots region of NO<sub>2</sub> is thermal power plants, urban cities, and industrial regions. In addition to NO<sub>2</sub>, carbon monoxide (CO) is also an important trace gas in

the troposphere and is the main precursor of secondary pollutant ozone in  $\text{NO}_x$ -rich environments. Though CO is not a direct greenhouse gas, it has a global warming potential because of its effects on the lifetime of several greenhouse gases. The natural and anthropogenic sources of CO are forest fire, biofuel burning, volcanic activities, and incomplete combustion of fossil fuels, oil, coal, wood, natural gas, and oxidation of hydrocarbons. However, a significant amount of contribution to CO is from anthropogenic emissions. Harmful effects of CO are dizziness, headaches, stomachache, confusion, tiredness. CO is a tracer of air pollution due to its lifetime of about ~1-2 months (Drummond et al., 1996).

Natural and anthropogenic activities are responsible for aerosol in the atmosphere. Anthropogenic activities over South Asia have caused considerable changes in aerosol composition and loading. Fine mode aerosol ( $\text{PM}_{2.5}$ ) is mainly from gas to particle conversions which are from biogenic and anthropogenic emissions. Coarse mode aerosol (particles with a diameter larger than 10  $\mu\text{m}$ ) arise from natural sources namely deserts, oceans, volcanoes, and biosphere with less contribution from anthropogenic activities. Over the ocean surface, the natural global aerosol mass is controlled by sulphate, sea salt, and dust aerosol (David et al., 2018). Further, aerosol also affects the earth-atmospheric radiation budget directly in scattering and absorption of incoming solar radiation and indirectly as clouds formation and precipitation (Ramachandran and Kedia, 2013). Thus, aerosol can influence the Indian monsoon (David et al., 2018).

Earlier studies indicate that vehicular emissions (Mahalakshmi et al., 2014, 2015), industrial and thermal power plant emissions (Ramachandran et al., 2013) contribute significantly to atmospheric pollution, including gaseous pollutants. The ambient air quality is largely determined by the concentration of trace gases and particulate matter in the atmosphere (Nishanth et al., 2014). An increase in the concentration levels of trace gases and particulate matter has been a challenging environmental issue in urban and industrial areas. Numerous studies have been attempted across the globe to understand the air pollution concentrations during the lockdown period and results indicate the varied range of percentage reductions in pollutant concentrations. These studies are based on ground-based measurements alone (Mohato and Ghosh, 2020; Mor et al., 2020) or satellite data alone (Biswal et al., 2020; Xu et al., 2020) or with a combination of ground measurements and satellite data (Ratnam et al., 2020; Biswal et al., 2021; Singh and Chauhan, 2020). Biswal et al. (2021) reported lockdown induced changes in tropospheric  $\text{NO}_2$  variability over the urban and rural regions of the Indian sub-continent with a marked reduction of 30-50 % over the urban and megacities. This change was mainly attributed to the reduced traffic emissions due to restrictions on travel. In contrast to the above, an increase in levels of air pollutants during lockdown is also noticed in certain regions, which are associated with natural emissions (dust storms, forest fires) and prevailing meteorological conditions. During India's phase-I of lockdown (25<sup>th</sup> March 2020 – 7<sup>th</sup> April 2020), Ratnam et al.

95 (2020) showed a decrease of Aerosol Optical Depth (AOD<sub>550</sub>) over the Indo-Gangetic plains (IGP) region and a drastic increase over central India, which were mainly due to the absence of anthropogenic activities and dominance of natural sources respectively. However, the above said studies have not carried any detailed statistical analysis to indicate the significant changes are due to the imposed lockdown besides the long-term variability.

100 The objective of the present study is to understand the air quality quantitatively over the Indian region under the control measures related to COVID-19 restrictions in the country. Thus, the present study examined the spatio-temporal variations of remotely sensed Tropospheric columnar NO<sub>2</sub> (TCN), Tropospheric columnar CO (TCC) and Aerosol Optical Depth (AOD<sub>550</sub>) during LD and pre-LD and compared with the preceding year (2019) and short-term mean (2014 – 2020). The present study reported lockdown-induced changes on TCN, TCC, and AOD<sub>550</sub> over the Indian region with special emphasis on the hotspot (usual predominant sources), and urban regions. Further, to study the lockdown-induced changes besides the inter-annual variability, statistical analyses were carried out to assess the influence of India's strict lockdown on these pollutants. To distinguish natural and anthropogenic emissions, we attempted to correlate the subsequent changes associated with meteorology, long-range transport as well as forest fires.

## 2. Data

110 Satellite measured air pollutants data offer reliable, uninterrupted observations with high spatial and temporal coverage than ground-based measurements which are point observations. Thus, the TCN observations from the Sentinel-5P/Tropospheric Monitoring Instrument (S5P-TROPOMI) and Aura/Ozone Monitoring Instrument (Aura/OMI), TCC data from high spatial resolution TROPOMI, AOD<sub>550</sub> data from Moderate Resolution Imaging Spectroradiometer (MODIS) Terra/Aqua platforms are used in the present study. The brief 115 details of these sensors are given in Table 1. The TROPOMI was launched on 13<sup>th</sup> October 2017 as the single payload onboard the S5P satellite of the European Space Agency (ESA) has nadir-viewing spectral range covering wavelength bands between the ultraviolet and the shortwave infrared. TROPOMI is a push-broom imaging spectrometer flying in a sun-synchronous orbit at 824 km altitude and is designed to retrieve the concentration of several atmospheric constituents which include TCN, TCC, SO<sub>2</sub>, etc. TROPOMI retrieved TCN and TCC values 120 with quality flag greater than 0.50 are considered in the present study (Eskes et al., 2019). It was developed jointly by ESA and Royal Netherlands Meteorological Institute (KNMI), which is the most advanced multispectral imaging spectrometer (Alonso et al., 2020). OMI was successfully launched on the National Aeronautics and Space Administration's (NASA's) on Earth Observing System Aura Satellite is a push broom ultraviolet/visible spectrometer that measures the Earth's backscattered radiance and solar irradiance. Aura/OMI has a swath width

125 of 2600 km with a nadir field-of-view, at a spatial resolution of  $0.25^\circ \times 0.25^\circ$  giving daily global 30 % Cloud-Screened TCN level 3 product (present study used Version 3) and crossing the equator at 13:45 local time (Krotkov et al., 2017). The MODIS sensor onboard NASA's two Earth Observing System Terra and Aqua platforms are providing AOD retrievals.

Parameter	Data source	Resolution	Website
TCN	Aura/OMI Sentinel-5P/TROPOMI	$0.25^\circ \times 0.25^\circ$ (version: V003) $3.5 \times 7 \text{ km}^2$ (year, 2019; version: 01.02.02 & 01.03.00) & $3.5 \times 5.5 \text{ km}^2$ (year, 2020; version: 01.03.02)	<a href="https://earthdata.nasa.gov/">https://earthdata.nasa.gov/</a>
TCC	Sentinel-5P/TROPOMI	$7 \times 7 \text{ km}^2$ (year, 2019; version: 01.02.02 & 01.03.00) & $5.5 \times 7 \text{ km}^2$ (year, 2020; version: 01.03.02 )	<a href="https://earthdata.nasa.gov/">https://earthdata.nasa.gov/</a>
AOD	MOD08_D3 from Terra & MYD08_D3 from Aqua	$1^\circ \times 1^\circ$ (version: v6.1)	<a href="https://ladsweb.modaps.eosdis.nasa.gov/">https://ladsweb.modaps.eosdis.nasa.gov/</a>
Fire count	VIIRS	375 m	<a href="https://firms.modaps.eosdis.nasa.gov/download/create.php">https://firms.modaps.eosdis.nasa.gov/download/create.php</a>
Winds and Relative Humidity	ECMWF-ERA5 reanalysis	$0.25^\circ \times 0.25^\circ$	<a href="https://cds.climate.copernicus.eu/cdsapp#!/dataset/reanalysis-era5-pressure-levels?tab=form">https://cds.climate.copernicus.eu/cdsapp#!/dataset/reanalysis-era5-pressure-levels?tab=form</a>
<i>Reference Period: Jan-July (2014 – 2020); Strict Lockdown Period: 25<sup>th</sup> March – 3<sup>rd</sup> May 2020</i>			

**Table 1: Data resources**

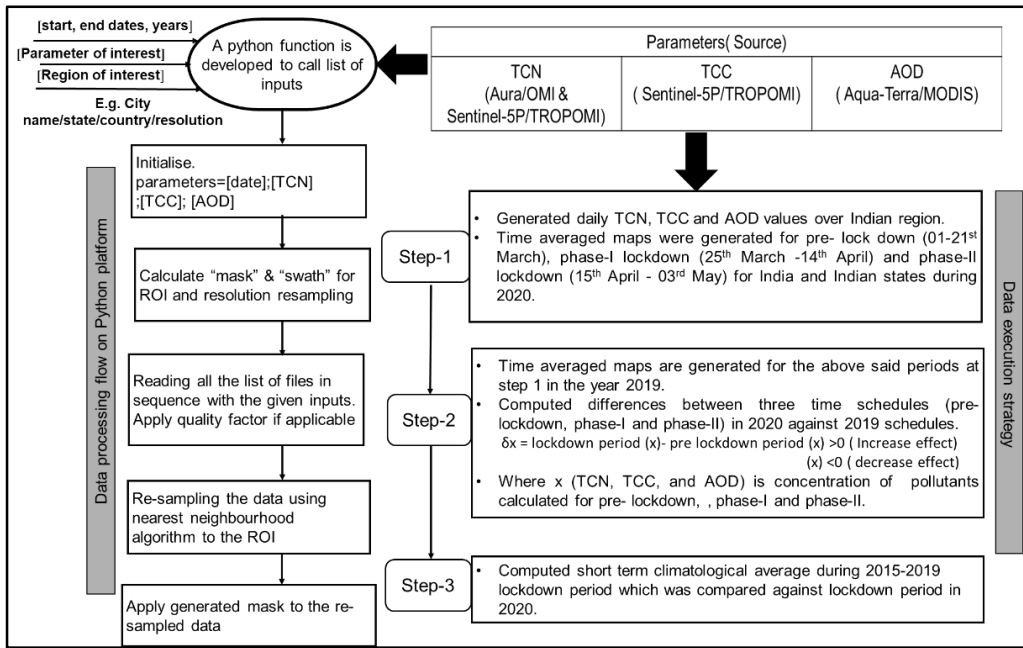
130 Daily level 3 (version: V003) TCN data was obtained from Aura/OMI for computing the short-term mean of TCN from 2015-2019 ([https://disc.gsfc.nasa.gov/datasets/OMNO2d\\_003/summary](https://disc.gsfc.nasa.gov/datasets/OMNO2d_003/summary)). However, high spatial resolution TCN and TCC data (Level 2) from TROPOMI is used during the LD period of 2020 and the equivalent period in 2019 (<http://doi.org/10.5270/S5P-s4ljg54>). The daily gridded global AOD product (Level 3) from Terra (MOD08\_D3\_v6.1) Aerosol Optical Depth at 550 nm, (Deep Blue algorithm, Land-only) and Aqua (MYD08\_D3\_v6.1) Aerosol Optical Depth at 550 nm (Deep Blue algorithm, Land-only) platforms were used to 135 investigate the aerosol loading over the Indian region for above said period. Detailed information about OMI sensor and MODIS sensor onboard Aqua/Terra platforms is explained by Li et al. (2020). Overland, the previous studies reported that MODIS-derived AOD uncertainty with respect to the Aerosol Network (AERONET) is  $\pm 0.05 \pm 0.20 \times \text{AOD}_{\text{AERONET}}$  (Sayer et al., 2013; Levy et al. 2013). Details of MODIS AOD retrieved algorithm for

140 collection 6.1 and its validation can be found in Hsu et al., (2019) and Sayer et al., (2019) respectively. In addition to the above datasets, fire counts data from Visible Infrared Imaging Radiometer Suite (VIIRS) with confidence > 80% were used. To understand the role of meteorology, winds from European Centre for Medium-Range Weather Forecasts (ECMWF- ERA5) reanalysis which gives hourly data at different pressure levels (700 hPa and 850 hPa) was also used in the present study. Similarly, relative humidity from ECMWF for the respective pressure  
145 levels is also used.

### 3. Methods

In the present study, we attempted to assess the impact of lockdown on air quality over India by examining remotely sensed daily concentrations of TCN, TCC, and AOD<sub>550</sub> from January 2014 to October 2020.  
150 Further, daily concentrations of the above said parameters were de-trended during the study period to subside the long-term changes. Hence, phase-wise changes in TCN, TCC levels, and AOD<sub>550</sub> could be attributed to LD-induced changes. Thus, the present study focused on the air pollution over the Indian region, its states, and its capital city during the strict lockdown periods (phase-I and phase-II). Analysis of satellite-based observations of TCN from the years 2015 to 2020, TCC during 2019-2020, and AOD<sub>550</sub> from 2014-2020 was carried out for  
155 lockdown period (phase-I and phase- II) as well as pre-lockdown period. Short-term climatological means during pre-LD, phase-I, phase-II were computed for TCN from 2015 to 2020 and AOD<sub>550</sub> from 2014 to 2020 to assess the temporal changes of pollutants in the atmosphere. We have focused our analysis on the first two phases of lockdown in which the industrial and transport sectors were brought to a near standstill.

Figure 1 shows the data processing and execution strategy followed in this study. The detailed  
160 methodology used in this study is as follows. Python programming language is used to analyse TCN, TCC, and AOD<sub>550</sub> variables during the study period as discussed in Figure 1. The parameters TCN, TCC, and AOD<sub>550</sub> are extracted from the respective source files considering quality flags ([https://github.com/aarathimuppalla/airpollution\\_ld\\_study.git](https://github.com/aarathimuppalla/airpollution_ld_study.git)). Swath and mask are calculated for the region of Interest and the data is resampled using the nearest neighbour algorithm. Further, time-averaged maps of TCN,  
165 TCC, and AOD<sub>550</sub> for pre-lockdown, phase-I, and phase-II lockdown were generated for the years 2020 and 2019 along with difference maps. With respect to 2020, if the difference in pollutant concentrations ( $\delta x$ ) is greater than zero indicating an increased effect and vice versa. Short-term climatological means of TCN for the years 2015 - 2020 and AOD for the years 2014 - 2020 were computed. Thereafter, the regional increase/decrease in pollutant concentrations over the country and individual states were analysed.



170

**Figure 1: Data processing steps and methodology**

### 3.1 Statistical metrics

Further, detailed statistical metrics for TCN, TCC, and  $\text{AOD}_{550}$  namely mean, standard deviation (SD), percentage of the number of positive and negative pixels, and student's paired t-test values were computed. To estimate metrics from the long-term data against lock period in 2020, here we utilized TCN data obtained from OMI and 175 AOD<sub>550</sub> from MODIS. These metrics are calculated for every week starting from 1<sup>st</sup> January to 31<sup>st</sup> July as 31 weeks in total for the years 2015-2020 for TCN and 2014-2020 for AOD<sub>550</sub> over the Indian region. Thus, the following steps were implemented to quantify the metrics. These steps are written for TCN as an example.

$$b_{2020-2019} (\text{TCN}) = \text{TCN} (2020) - \text{TCN} (2019) \quad (1)$$

$$b_{2020-2015 \text{ to } 2019} (\text{TCN}) = \text{TCN} (2020) - \text{TCN} (2015 - 2019) \quad (2)$$

180

$$1\text{SD} = \sqrt{\sum_{i=1}^N \frac{(b_i - \mu_b)^2}{N}} \quad (3)$$

$$\text{If } \begin{cases} b_i > 1\text{SD}, \text{ positive pixels } (P_p) \\ b_i < -1\text{SD}, \text{ negative pixels } (N_p) \\ -1\text{SD} \leq b_i \leq 1\text{SD}, \text{ neglect pixels} \end{cases} \quad (4)$$

185 Where  $N$  is the total number of qualified pixels over the Indian region and  $\mu_b$  is mean bias. At each pixel, weekly bias ( $b$ ) of TCN is estimated from the weekly mean TCN during the 2020 lockdown period w.r.t 2019 and 2015-2019 period as shown in equations (1-2). For prominent change detection, additionally, 1SD deviation filter was applied on the bias values of TCN and  $AOD_{550}$ . Therefore, if bias is greater than 1SD then the featuring pixels are classified as positive and if less than -1SD then they are considered as negative pixels. Pixels within  $\pm 1\text{SD}$  are omitted to avoid minimalistic feature changes and for better characterization. Subsequently, we computed the percentage of positive (Increased area) and negative pixels (decreased area) using the following equations (5-6).

190

$$\% P_p = \frac{\text{count}(P_p)}{N} \times 100 \quad (5)$$

$$\% N_p = \frac{\text{count}(N_p)}{N} \times 100 \quad (6)$$

195 The same equations were applied on  $AOD_{550}$  during the 2014 - 2020 study periods. Further to understand LD-induced changes in TCN and  $AOD_{550}$  quantitatively daily mean values are de-trended using yearly data, which accounts for long-term changes in TCN and  $AOD_{550}$  respectively. De-trended values of TCN and  $AOD_{550}$  are generated by subtracting the linear regression estimated values from the daily values of TCN and  $AOD_{550}$ . To study the lockdown-induced changes with significant levels, a paired t-test (Freedman et al., 2007) was implemented on the de-trended TCN and  $AOD_{550}$  data during the respective study period. The t-test follows a

200 Student's t-distribution under the null hypothesis of  $H_0$  with the means ( $\mu$ ) of two populations are equal ( $\mu_1 = \mu_2$ ) with alternative hypothesis  $H_a: \mu_1 \neq \mu_2$ . To reject or accept the null hypothesis, p-value was used in this study. The hypothesis  $H_0$  is rejected when a p-value is less than 0.05 and accepted if p-value is greater than 0.05 (5 % significance level).

#### 4. Results and Discussion

205 The present study analysed the satellite-based TCN, TCC, and  $AOD_{550}$  data to assess the lockdown-induced changes over the Indian region.

#### 4.1 Effect of Lockdown (LD) on TCN

The Spatio-temporal variability in TCN concentrations during the pre-lockdown and lockdown period (phase-I and phase-II) were analysed for the years 2019 and 2020 using high spatial resolution (Table 1) TROPOMI. Temporally averaged concentrations of TCN during pre-LD (01<sup>st</sup> March to 21<sup>st</sup> March 2020), phase-I and phase-II of lockdown, and the corresponding period of the previous year (2019) are shown in Figures 2a-c, along with the differences in concentration levels between different periods. During the pre-LD time of years 2019 and 2020 as shown in Figure 2a, the extent of TCN hotspot regions (majorly Eastern and National Capital region) remain same however, a mild reduction of TCN was noticed during pre-LD of 2020 compared to 2019. This could be probably due to inter-annual variability in TCN levels and also the absence of source emissions due to lockdown imposed by neighbouring countries via long-range transport (For example lockdown imposed in China from 23<sup>rd</sup> January 2020, Italy from 21<sup>st</sup> February 2020, and Malaysia from 18<sup>th</sup> March 2020). During this period, Biswal et al., (2021) reported similar reduction of TCN over NCR and other cities across the globe (Tian et al., 2020; Xu et al., 2020; Berman and Ebisu, 2020; Collivignarelli et al., 2020; Jephcote et al., 2021).

The mean TCN over the entire country during phase-I of 2020 and 2019 are  $1.53 \times 10^{15}$  and  $1.86 \times 10^{15}$  molecules cm<sup>-2</sup> respectively. A reduction of about 22 % TCN levels is observed in 2020 compared to 2019 during phase-I, which accounts for both inter-annual variability and lockdown-imposed changes. Further to understand the lockdown-induced changes in TCN levels, this study was focused on TCN hotspots, which includes power plants and metropolitan cities with industrial and transport activities. To contain the spread of COVID-19, about 95 % of the anthropogenic activities were halted (Ratnam et al., 2020) during phase-I LD. However, during phase-I, a few anthropogenic emissions are present under essential services (such as pharma industries, power plants, medical services, vehicles that were carrying daily commodities) and indoor emissions. As a result, the TCN levels and their area of extent as shown in Figure 2b during phase-I of LD in 2020 over the hotspot regions (Eastern region of India) decreased by 22 % when compared to an equivalent period of 2019. The eastern region of India has a significant number of major power plants and refineries with associated industries. During phase-I LD in 2020, a reduction of TCN levels is observed over this region, which is due to the shutdown of industries and urban activities such as transport and small-scale industries. However, the country's high TCN levels are noticed in the eastern region with less spread indicating the active role of power plant industries located in this region. Simultaneously, the National capital region (NCR) shows a marked reduction by about ~70 % during phase-I LD. The major source of emissions in the NCR is dominated by heavy traffic, densely located industries, and industries of steel, cement, and sugar (Garg et al., 2002; Ghude et al., 2008). As mentioned above, India's strict lockdown

permitted only essential services therefore remaining all activities were halted during the phase-I period. Thus, resulted in low levels of TCN over the hotspot regions except in the eastern region and a few grids of central western region due to continuous operation of power plants and petroleum refineries (Biswal et al., 2021).

To sustain the Indian economy, activities namely agricultural practices and associated activities (crop residue burning) were permitted during phase-II along with phase-I restrictions. Figure 2c shows TCN levels and their difference map during phase-II LD. With respect to the same period of phase-II in 2019, the TCN levels over the country decreased by 13 % with a mean TCN of  $1.55 \times 10^{15}$  molecules  $\text{cm}^{-2}$  and  $1.75 \times 10^{15}$  molecules  $\text{cm}^{-2}$  in 240 2020 and 2019. Thus, a continued decrease of TCN levels is recorded over the hotspot regions. However, an increase of TCN also observed over the neighbouring regions of the eastern region indicating the dispersion of 245 TCN. In contrast to earlier, an increase in TCN levels over the northeast region could be due to seasonal biomass burning in this region. Thus, the mean TCN levels over the entire country is  $1.54 \times 10^{15}$  molecules  $\text{cm}^{-2}$  during total LD (phase-I and phase-II together) with a reduction of 18 % compared to the respective period in 2019 as well as 250 with respect to 5 years mean TCN.

Overall, the southern part of India reported fewer TCN values as compared to eastern and NCR regions (hotspot regions) during pre-LD, phase-I, and Phase-II. The hotspots over the southern part of India are not as dense as in the eastern and northern regions could be one of the reasons for its lower values. The southern part of 255 India is comparatively hot and humid which will lead to high OH (hydroxyl) radicals concentrations than the Northern part of India. As a result, photolysis of  $\text{NO}_2$  will increase which results in low  $\text{NO}_2$  concentrations. Further, in south India, the number of large point sources, amount of biomass burning, and vehicular population are less compared to the Northern part of India (Ghude et al., 2008). Thus, reduced TCN levels over the southern part of India irrespective of LD were observed due to the above facts. Weekly variations of TCN were also shown 260 in Figure 2d to assess the extent of source emission during the lockdown period. Therefore, the present study depicted the possible driving factors of TCN values during pre-LD, phase-I, and phase-II using high-resolution spatial data from the satellite.

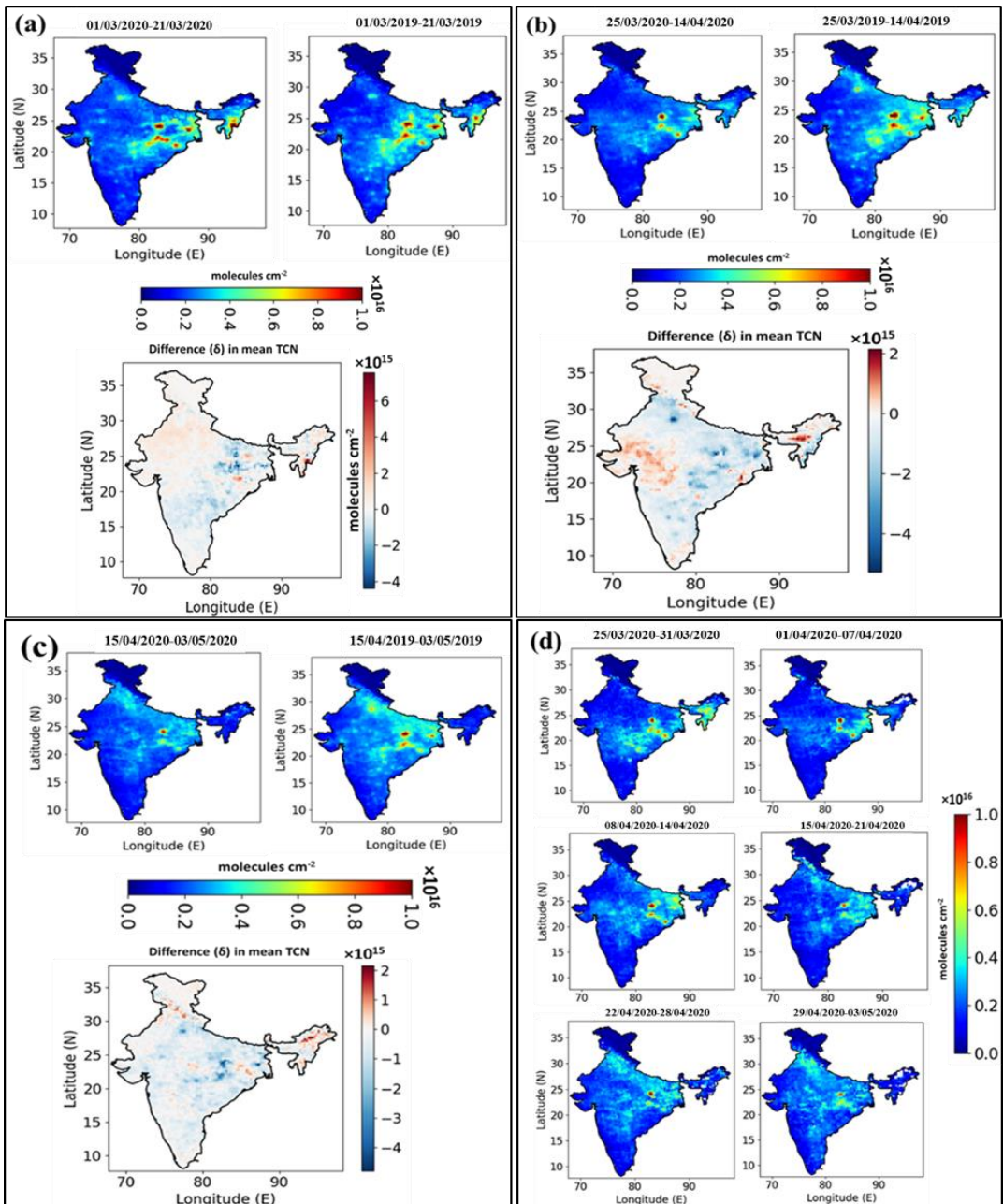


**Figure 2: Time-averaged TROPOMI TCN concentration and their difference maps between 2020 and 2019 during a) pre-LD b) phase-I lockdown c) phase-II lockdown d) weekly mean TCN variation starting from 25<sup>th</sup> March to 03<sup>rd</sup> May 2020.**

#### 4.1.1 Short-term climatological variations in TCN due to lockdown

Time series analysis of TCN was carried out during 2015 - 2020 for January to July over the entire Indian region covering cold and hotspot regions as shown in Figures 3a-d. A smoothing function with a span of 7 days was used for better visualization of patterns/trends in TCN levels as shown in Figures 3a-b, with red (green) bars indicating increase (decrease) TCN levels in 2020 relative to 2019 and mean of 2015-2019. The 7-day moving average shows a significant decrease of TCN concentration with a 99.99% (p-value << 0.05) confidence interval during the total lockdown period. However, it is also noticed that a decrease of TCN during prior and post lockdown periods, which is further tested statistically and found insignificant change with p-values of 0.08 and 0.24 respectively.

Further statistical significance of TCN variability across hotspot, cold spot regions, and also over the major cities where TCN dropped (↓) drastically (except NE which showed increase) along with their percent drop during total LD when compared to 5 year mean TCN levels were summarized in Table 2. It clearly shows the TCN levels over the IGP (22% ↓), eastern region (29% ↓), and major cities (New Delhi 54% ↓) declined significantly compared to the preceding 5 year mean TCN levels during the total LD period. Change in TCN during the study period is also associated with the inter-annual and seasonal variability besides its dominant anthropogenic sources. Figure 3c shows the annual means of TCN in pre-LD, phase-I, and phase-II LD during 2015-2020 period. It depicts inter-annual variability in TCN between the years at each time scale along with the lockdown-imposed changes. Between the time scales during the study period, a clear seasonality in TCN levels is also observed in Figure 3c.

The horizontal bar plots in Figure 3d show the rate of change (RoC) in TCN levels in 2020 against the mean during 2015-2019 indicating the impact of lockdown on TCN concentrations over the Indian region. The RoC is extremely important in weather and climatological studies because it allows understanding and predicting the trends/patterns in climatic parameters. RoC is used to describe the percentage change in a parameter over a defined time period and it represents the rate of acceleration of the parameter. To compute the RoC in this study, we have used de-trended TCN daily values, which account for long-term variability in TCN. Thus, the present RoC depicts the TCN variability due to the lockdown-imposed changes alone. There is an observable lowering in TCN levels relative to the short-term climatological mean by 12% for the pre-lockdown period as Lal et al., (2020) also reported similar results. During the period from January-April 2020, authors reported a substantial reduction in the level of TCN, TCC, and AOD<sub>550</sub> across the globe during the COVID-19 pandemic as each country (at different spatial scale) imposed lockdown at different time scales. This could be the reason for a reduction in concentrations of TCN during the pre-LD period in 2020 as compared with 2019 as well as the mean picture of 2015-2019. Furthermore, a noteworthy reduction of TCN concentration by 18% and 15% is observed for the phase-I and phase-II lockdowns respectively over the Indian region.

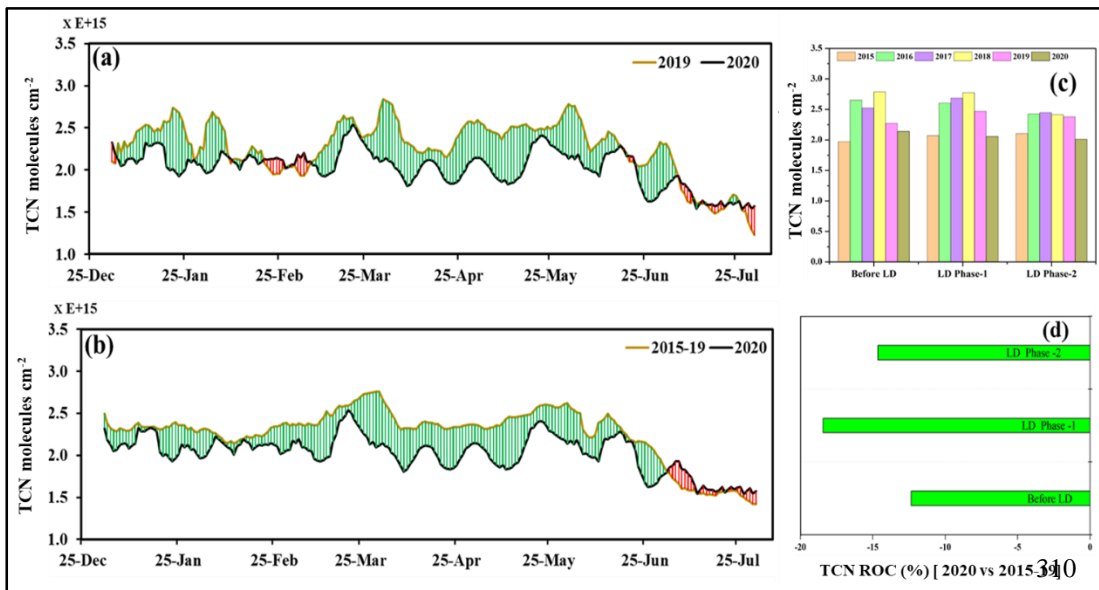


**Figure 3: Moving average time series analysis during January-July of TCN during a) 2019 vs. 2020 b) short-term climatological mean of TCN (2015-2019) vs. 2020 c) Annual variations of TCN (2015-2020) during period of before lockdown and different phases of lockdown and d) Rate of change of TCN during 2020 w.r.t. 2015-2019 period.**

315

Region/City	*Student's Paired t-test p-value (RoC in percent during Total LD)		
	Pre-LD	During total LD	Post LD
IGP	0.03	<< 0.05 (22 % ↓)	0.31
East	0.62	<< 0.05 (29 % ↓)	0.11
NE	0.66	0.19 (3 % ↑)	0.55
New Delhi	0.57	0.0002 (54% ↓)	0.05
Bangalore	0.58	2.62E <sup>-5</sup> (43% ↓)	0.17
Chennai	0.37	0.012 (41% ↓)	<<0.05
Mumbai	0.95	0.011 (35% ↓)	0.17
Hyderabad	0.49	0.0003 (30% ↓)	0.007

\* p-value < 0.05 is significant and vice-versa; (↓, ↑) indicates (decrease, increase)

**Table 2: Student's paired t-test for TCN during the lockdown period against 5-year mean (2015-2019)**

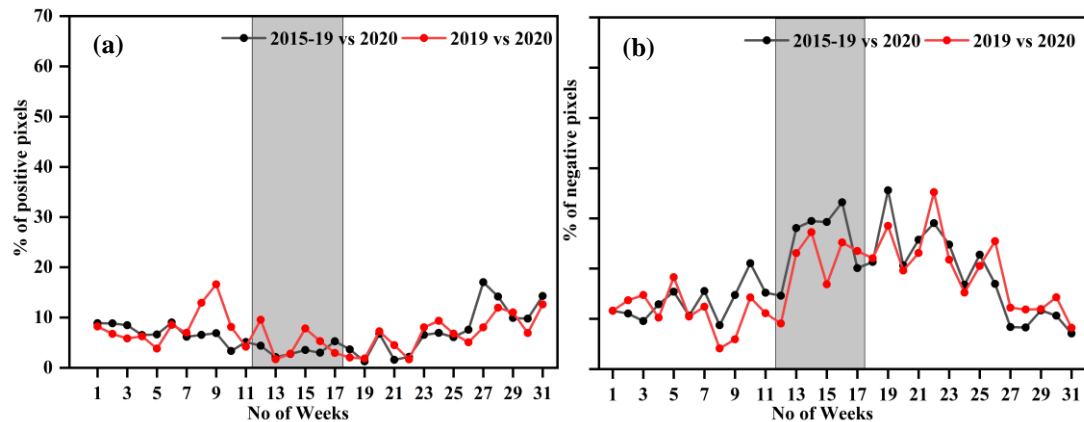


**Figure 4: OMI measured TCN a) percentage of positive pixels b) percentage of negative pixels during the period 2020 vs (2015-19) and 2020 vs 2019.**

330

Figures 4a-b show statistically computed TCN metrics for a number of positive pixels and number of negative pixels in percentage during January to July period on a weekly interval which starts from 01<sup>st</sup> January. Weekly TCN means for the year 2015-2019, 2019 and 2020 were used to calculate positive and negative pixel count based on methodology stated in section 3.1. Thus, the red color line in Figures 4a-b represents the number of positive/negative pixels for the years 2019 vs. 2020 and the black color line represents the same for the years 335 2015-2019 vs 2020. The study showed a greater number of negative pixels (decreased area) during lockdown weeks and vice-versa for positive pixels which depict the extent of area affected due to LD and subsequent changes in air pollutants over the Indian region.

340

#### 4.2 Effect of LD on TCC

The mean TCC levels over the Indian region during the pre-lockdown and LD periods were studied to assess the COVID-19 lockdown-induced changes in TCC. Figures 5a-c show mean concentrations of TCC over the Indian region during pre-LD, phase-I, and phase-II LD periods using TROPOMI data. During the pre-lockdown period 345 (01-21<sup>st</sup> March 2020), TCC levels were higher (mean =  $2.39 \times 10^{18}$  molecules cm<sup>-2</sup>) as compared to 2019 by ~ 4.8%, which indicates the increasing effect of anthropogenic activities and inter-annual variability. As shown in Figure 5b difference map, the TCC levels increased in the north-eastern (NE) region followed by part of central India (CI) and south of north-west (S-NW) of India as compared to 2019 of phase-I LD period. An observed

increase over these regions was evaluated statistically and found insignificant ( $p > 0.05$ ). An increase of TCC in  
350 the NE region of India is mainly attributed to the active fire counts (Figure 5d) during phase-I of LD as shown in  
Figure 5b. During phase-I, other regions of India namely the IGP, north, and south regions show decreased TCC  
levels compared to the same period of 2019. The decreased TCC levels in these regions during phase-I are  
attributed to the shutdown of industries (cement, sugar, and steel, etc.), absence of transportation and restriction  
on crop residue burning. However, household emissions due to residential cooking are still present during  
355 lockdown which is a major contribution to CO from rural areas and some parts of the urban region (slums). In  
India, 72 % of the population live in rural and urban slums and most of them are continued to use household  
biofuel for cooking under lockdown (Verma et al., 2018; Beig et al., 2020).

However, the mean TCC levels as shown in Figure 5c are higher during phase-II of lockdown. Over the  
entire country, the mean TCC value during phase-II is  $2.38 \times 10^{18}$  molecules  $\text{cm}^{-2}$  in comparison to the 2019 mean  
360 value of  $2.32 \times 10^{18}$  molecules  $\text{cm}^{-2}$ . In phase-II of LD, the TCC levels are decreased in the NE region, which is  
strongly attributed to the reduced active fire activity in this region as shown in Figure 5c. Except in the NE region,  
a consistent increase of TCC levels is observed during phase-II. Since the agriculture farming industry is  
exempted in the phase-II LD and observed active fire counts in central India, thus observed enhancement in the  
365 TCC levels during phase-II. An increase or decrease of TCC levels in the atmosphere is mainly dominated  
significantly by anthropogenic activities compared to natural emissions (Kanchana et al., 2020) as discussed  
earlier. However, comprehensive reasons for the increase of TCC levels in phase-II are not investigated in this  
study.

370

375

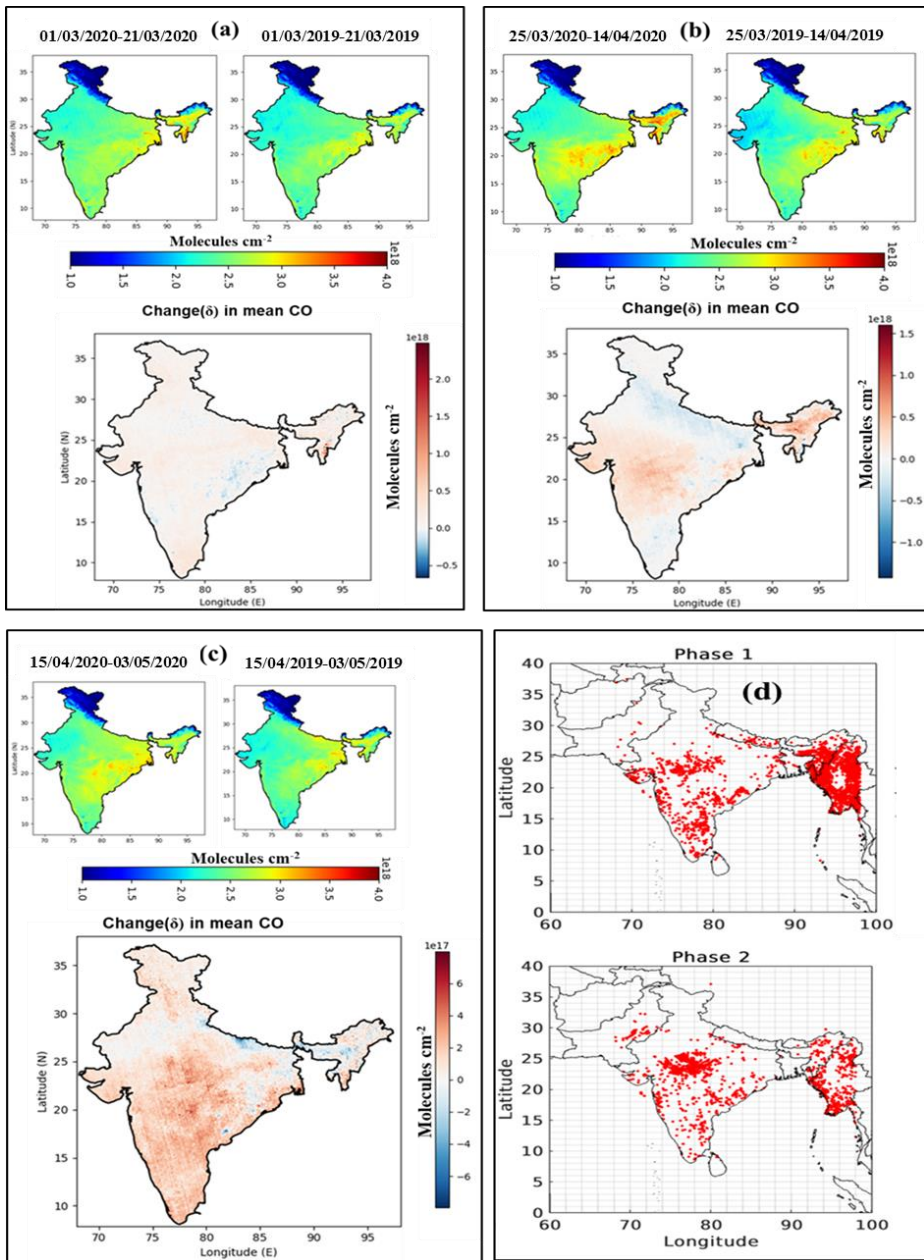


**Figure 5: TROPOMI derived Time averaged TCC concentration and their difference maps in 2020 and 2019 a) pre-LD b) phase-I lockdown c) phase-II lockdown d)Fire counts from VIIRS for phase-I, phase-II during 2020.**

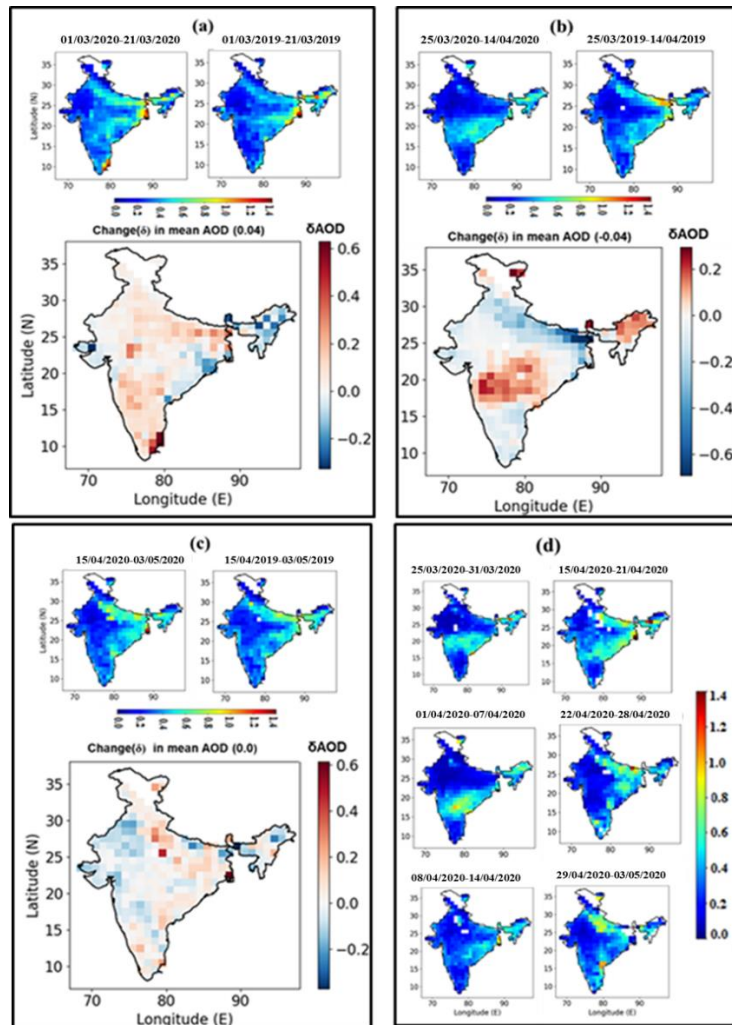
#### 4.3 Effect of LD on AOD<sub>550</sub>

385 We have used Terra-Aqua/MODIS derived AOD<sub>550</sub> during 2014-2020 for January to July to understand the lockdown-imposed changes. Terra/MODIS AOD<sub>550</sub> represents the footprint for 10:30 and Aqua/MODIS AOD<sub>550</sub> for the 13:30 local time. As we observed similar spatial variation of AOD<sub>550</sub> from both Terra-Aqua/MODIS, only  
390 Aqua/MODIS derived AOD<sub>550</sub> is shown here (Figure 6). AOD<sub>550</sub> levels over the Indian region for 2019, 2020, and the difference in AOD<sub>550</sub> for both years for the pre-lockdown period are depicted in Figure 6a. During this period, the AOD<sub>550</sub> levels for 2020 over the IGP region (~21% of the Indian Territory landmass) are more compared to the rest of the regions of India which is expected throughout the year. This is mainly because of its orographic effect and densely populated (accommodating ~ 40% of the Indian population). The main anthropogenic sources over the IGP region are coal-based power plants and industries, crop residue and forest fires, and household cooking which contribute to high AOD in this region. Thus, the IGP is known as the first  
395 hotspot for anthropogenic aerosol emission in South Asia. During phase-I of LD as shown in Figure 6b, aerosol loading over the IGP region attained its baseline concentration (~ 45% drop w.r.t. 2019 of the same period) due to the strict implementation of LD. This region is densely populated and congested industrial activities, which were shut down during this period resulted in a nearly AOD free atmosphere. This indicates an absence of anthropogenic activities due to mobility restrictions. Further, prevailing meteorology over IGP (high wind speed  
400 and low relative humidity at 850 hPa and 700 hPa) is also favoured for a decrease in AOD<sub>550</sub> during phase-I LD.

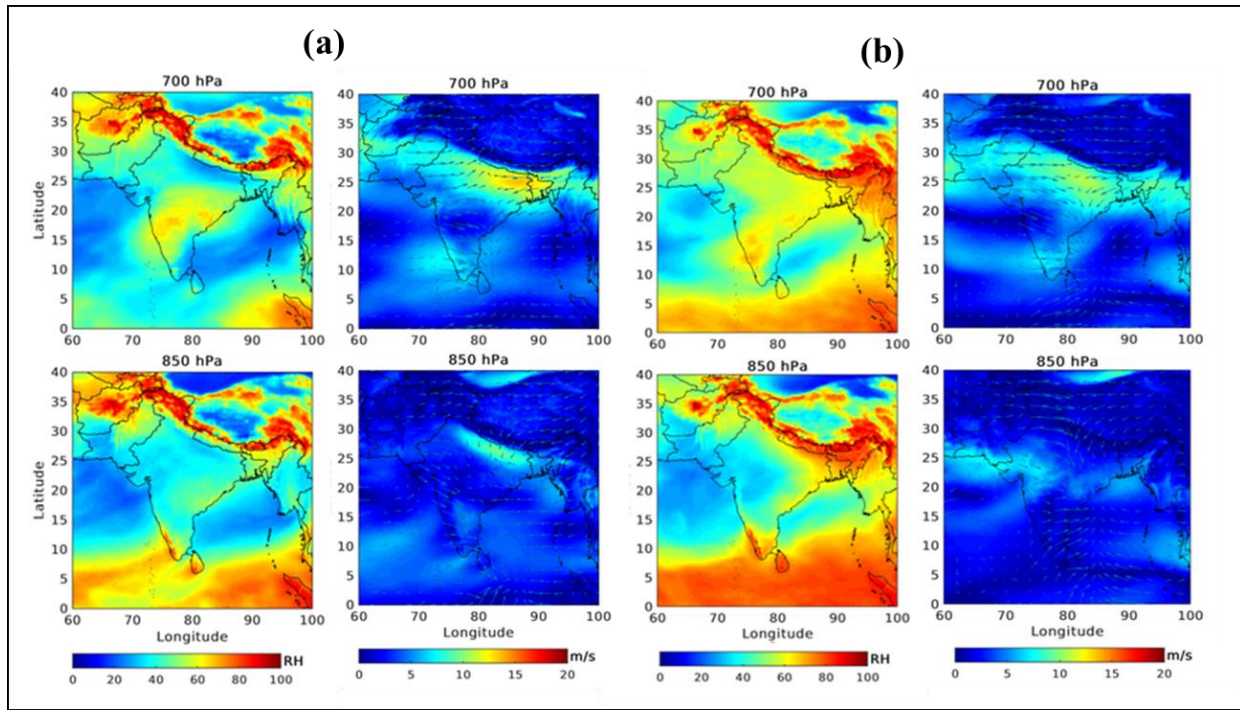
Despite the strict LD in the country, an unexpected increase in AOD<sub>550</sub> is observed by ~28 % compared to the preceding year of the same period over Central India (CI) which is predominantly dominated by dust storms (Ratnam et al., 2020) through long-range transport and prevailing meteorology (Pandey et al., 2020). Thus, to understand the prevailing meteorology over CI, phase-wise relative humidity and wind speed at pressure levels  
405 850 hPa and 700 hPa respectively were analysed as shown in Figures 7a-b. During phase-I and phase-II, the majority of the winds over CI are dominated by westerly (calm winds) with high relative humidity. Under this prevailing meteorology, calm winds contribute to slow dispersion and high Relative humidity (RH) modulates the aerosol chemistry and hygroscopic growth mechanism (Pandey et al., 2020). As a result, the increase of AOD<sub>550</sub> over CI is observed. Further, high AOD<sub>550</sub> over NE regions was also observed because of high active forest fire  
410 counts (Figure 5d) compared to the 2019 LD period. Figure 6c shows AOD<sub>550</sub> during phase-II of India's LD in 2020 against AOD<sub>550</sub> in 2019 of the same period. During this phase, an increase in AOD<sub>550</sub> (~ 3%) over IGP was observed. Over CI, a reduction of AOD<sub>550</sub> (~ 18%) was observed compared to phase-I of LD and not much change (~1%) when compared to the respective period in 2019 which depicts reversal of meteorology in phase-II with

respect to phase-I. Causative factors for this decrease over CI w.r.t phase-I are due to low RH and high wind speed  
415 at 700 hPa and 850 hPa over this region.

In a nutshell, this study demonstrates the lockdown induced Terra/MODIS AOD<sub>550</sub> changes over the IGP and CI during the total LD period shows a significant change with a p-value of 0.01 (99 % confidence interval) with a decrease of 20 % over IGP and 0.03 (97 % confidence interval) with an increase of 25 % over CI when compared to the equivalent period in 2019.



420  
**Figure 6: Aqua/MODIS derived Time averaged AOD<sub>550</sub> and their difference maps in 2020 and 2019 a) pre-LD b) phase-I lockdown c) phase-II lockdown d) weekly variation in total lock period during 2020.**



425 **Figure 7: Mean relative humidity (%) and mean winds ( $\text{ms}^{-1}$ ) observed at 700 hPa and 850 hPa (a) phase-I  
of lockdown and (b) phase-II of lockdown**

#### 4.3.1 Short-term climatological variation of $\text{AOD}_{550}$ due to lockdown

Aerosol optical depth is one of the important short-term climatic forcing agents along with long-lived greenhouse  
430 gases namely carbon dioxide ( $\text{CO}_2$ ), methane ( $\text{CH}_4$ ), water vapor ( $\text{H}_2\text{O}$ ), and nitrous oxide ( $\text{N}_2\text{O}$ ). A 7-day  
smoothing average filter was applied on  $\text{AOD}_{550}$  time series data as discussed in section 4.1.1. Figures 8a-d show  
a 7-day moving average time series analysis of  $\text{AOD}_{550}$  levels for MODIS Terra and Aqua from January to July  
over the Indian region for 2014-2019 mean values, 2019 and 2020.  $\text{AOD}_{550}$  measured by Terra/Aqua-MODIS  
(Figures 8b & 8d) show a significant change in aerosol loading over the country during the lockdown period in  
435 2020 compared to the mean  $\text{AOD}_{550}$  of 2014-2019. Statistical analysis of Student's paired t-test shows a strong  
significant change in  $\text{AOD}_{550}$  with a p-value of  $<<0.05$  for Terra/Aqua-MODIS during the total LD against 6-year  
mean (2014-2019). Interestingly the present analysis shows a very much significant change of  $\text{AOD}_{550}$  during post  
LD compared to LD with p-value  $<<<0.05$  (order of an Integer $\times 10^{-12}$ ), which attributes to the continued effect

of lockdown as phase-III and IV and scavenging effect during monsoon season. Due to the increase of  
440 precipitation in the active summer monsoon (June-July) season, lowering of aerosol is expected (Boucher et al., 2013). Thus, the continued lockdown and active monsoon improved the air quality beyond the strict lockdown period as shown in Figures 8a-d.

The annual mean  $AOD_{550}$  over the Indian region in each phase is shown as vertical bars in Figures 8e-f, indicating the inter-annual variability of  $AOD_{550}$  across the phases and seasonal modulation between the phases  
445 during 2014-2020. Despite inter-annual and seasonal variability of  $AOD_{550}$ , the strict lockdown in 2020 shows a decrease in phase-I and phase-II compared to pre-LD, which could be associated with the reduced anthropogenic sources besides prevailing meteorology as discussed in section 4.3. The RoC in  $AOD_{550}$  was computed (Figures 8e-f) to understand the effect of short-term climatological mean  $AOD_{550}$  over the lockdown period in 2020. A positive RoC of +8.8 % (+14%) was observed during pre-LD as measured by Terra/MODIS (Aqua/MODIS)  
450 against 6-year mean  $AOD_{550}$ . This increase is tested statistically and found insignificant with p-values of 0.11 and 0.37 for Terra/MODIS and Aqua/MODIS respectively. During phase-I (phase-II) Terra/MODIS showed statistically significant negative RoC with -24 % (- 9%) and Aqua/MODIS showed -22 % (-7%) against 6-year mean  $AOD_{550}$  as most of the sectors were turned off except household emissions and essential services. Therefore,  
455 this study reports, India's strict lockdown improved the aerosol air quality over the country with marked changes over the IGP and CI respectively.

460

465

470

475

480

485

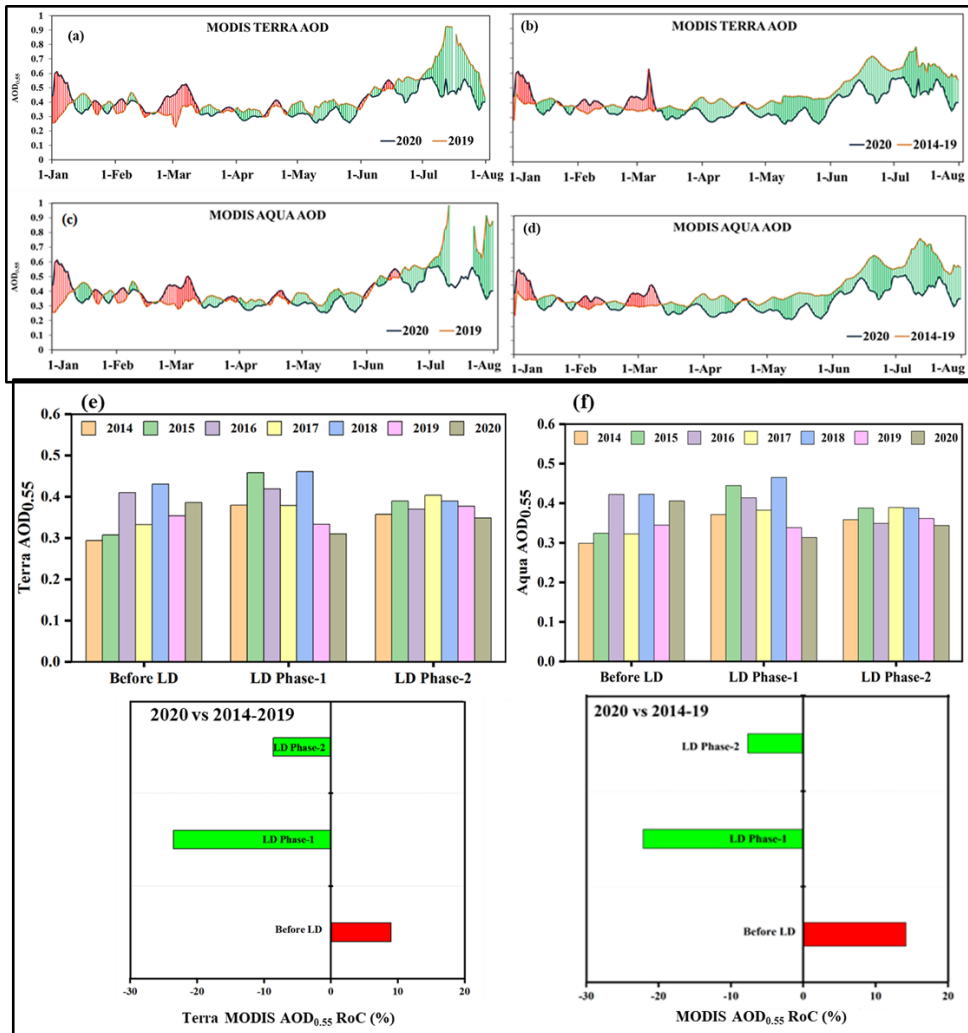
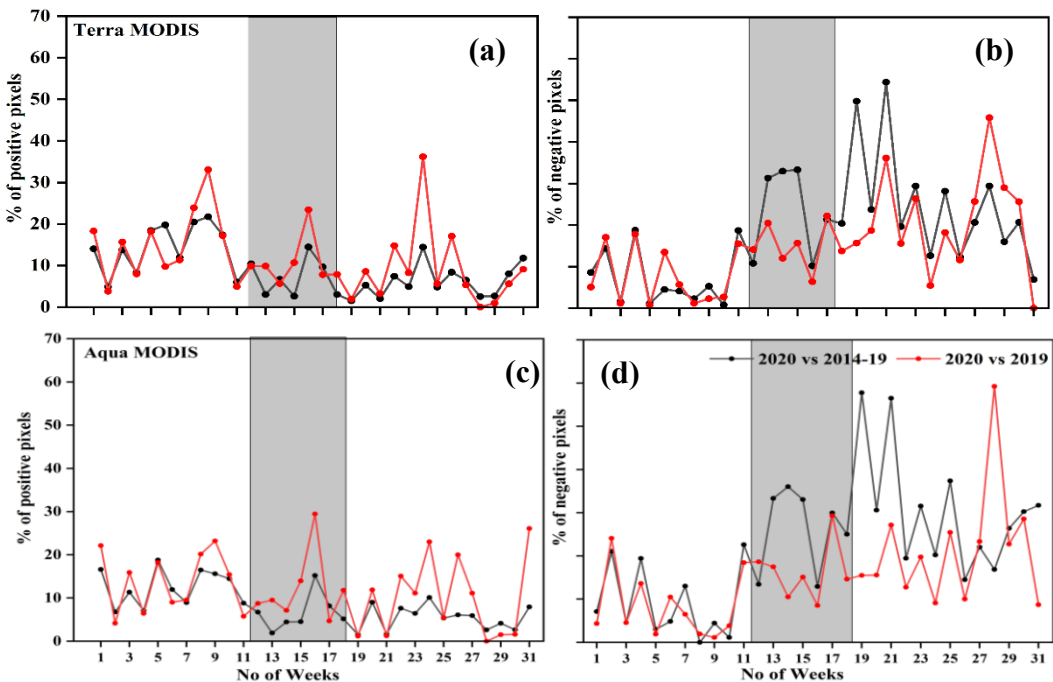


Figure 8: a) Moving average time series analysis of AOD<sub>550</sub> measured by Terra/MODIS during 2019 and 2020 b) Terra/MODIS short-term climatological mean of AOD<sub>550</sub> (2014-2019) vs. 2020 c) time series AOD<sub>550</sub> measured by Aqua/MODIS during 2019 and 2020 d) Aqua/MODIS short-term climatological mean of AOD<sub>550</sub> (2014-2019) vs. 2020 e) Variations of Terra/MODIS measured AOD<sub>550</sub> before Lockdown and different phases of Lockdown and respective RoC f) Variations of Aqua/MODIS measured AOD<sub>550</sub> before Lockdown and different phases of Lockdown and respective RoC.

Figures 9a-d show the number of positive and negative AOD<sub>550</sub> pixels in percentage at weekly intervals computed from the respective biases during the study period over the Indian region. Figures 9a-b show the percentage of positive and negative pixels of AOD<sub>550</sub> measured by the Terra/MODIS. During the lockdown weeks (shaded in grey color) in 2020, the number of positive pixels was less w.r.t 2019 and the short-term climatological mean of AOD. Figure 9b shows more percentage of the negative pixel during the same study period indicating the larger area of the extent with lower AOD<sub>550</sub> due to strict lockdown in India. This change is even high w.r.t short-term climatological mean of AOD<sub>550</sub>. The Aqua/MODIS-derived AOD<sub>550</sub> also shows similar variability and is as shown in Figures 9c-d.



**Figure 9: Terra/MODIS (a) percentage of number of positive pixels b) percentage of number of negative pixels during the period 2020 vs (2014-19) and 2020 vs 2019. Aqua/MODIS (c) percentage of positive pixels d) percentage of negative pixels during the period 2020 vs (2014-19) and 2020 vs 2019.**

#### 4.4 State wise Rate of Change (RoC) of TCN w.r.t. 2015-2019 and AOD w.r.t. 2014-2019

520 Table 3 show state-wise RoC computed for pre-LD, phase-I, phase II, and total LD phases in 2020 with respect to 5 year mean (2015-2019) for TCN and with respect to 6 year mean (2014-2019) for Terra/AOD<sub>550</sub> and Aqua/AOD<sub>550</sub>. A positive percentage of RoC indicates an increase of pollutants for the respective phases shown in Table 3 when compared to the same phase period of means of TCN for 2015-2019 and means of AOD<sub>550</sub> for 2014-2019. A negative percentage of RoC indicates the decrease of TCN and AOD<sub>550</sub> w.r.t 2015-2019 and 2014-525 2019 values respectively for the phases as shown in the Table 3. Results depict the change of pollutants over each state during the lockdown period compared to the respective period in 5 year mean for TCN and 6 year mean for both AOD<sub>550</sub>.

530 During the total lockdown period in 2020 w.r.t the mean of TCN during the same period for 2015-2019, the TCN values are dropped in the hotspot zones namely eastern states (Odisha, Chhatisgarh, and Jharkhand) and NCR regions (New Delhi, Ghaziabad, Faridabad, Gurugram, and Noida). Thus, the drop in TCN values over these regions is evaluated statistically and found a significant change. Similarly, the AOD<sub>550</sub> measured by the Terra-Aqua/MODIS also shows a strong reduction over the IGP region during the total LD. However, an unexpected increasing effect is noticed in the CI states with respect to 6 year mean of respect AOD<sub>550</sub> during phase-I. Similar results are also observed when compared to the preceding (2019) year mean AOD<sub>550</sub> which is discussed earlier 535 section in a detailed manner. Further, it is observed that the negative RoC of AOD<sub>550</sub> over the IGP region during phase-I is more prominent compared to phase-II RoC. It is also noticed further that the RoC of AOD<sub>550</sub> computed from the Terra-Aqua showing similar trends during the total lockdown period with a small difference in the amplitudes. This difference of amplitude between these two sensors could be due to a difference in overpass time, which changes atmospheric dynamics such as planetary boundary layer height, solar zenith angle, and prevailing 540 meteorology. An average of Terra /Aqua- MODIS derived RoC of AOD<sub>550</sub> shows a strong reduction in the western part of India mainly Rajasthan (-36 %) and Gujarat (-31 %) respectively during the total LD period (Ranjan et al., 2020). Therefore, in a nutshell, an analysis of RoC depicts regional variability of air pollutants during the total LD period in 2020 w.r.t to short-term (5-6 year) mean.

545

State Name	Pre-LD (%)			Phase-I (%)			Phase-II (%)			Total LD (%)		
	TCN	Terra/ AOD	Aqua/ AOD	TCN	Terra/ AOD	Aqua/ AOD	TCN	Terra/ AOD	Aqua/ AOD	TCN	Terra/ AOD	Aqua/ AOD
Andhra Pradesh	-15	-7	-6	-33	-30	-30	-23	6	-11	-28	-15	-22
Arunachal Pradesh	-14	-16	-3	8	14	21	13	-25	-51	8	4	1
Assam	-12	-13	-18	9	-10	-12	-3	-13	-29	2	-11	-19
Bihar	-4	20	30	-19	-54	-63	-16	-12	-24	-18	-34	-45
Chhattisgarh	-20	-1	1	-19	-5	-6	-18	24	15	-20	7	4
Gujarat	-1	-14	-24	-4	-33	-47	-15	-16	-27	-9	-25	-37
Haryana	0	11	18	-47	-39	-44	-21	-28	-41	-31	-34	-43
Himachal Pradesh	-13	35	-3	-36	-43	-50	-7	-9	8	-18	-28	-21
Jammu & Kashmir	13	4	13	12	3	1	-18	18	15	-3	10	7
Jharkhand	-14	21	-1	-30	-40	-39	-16	20	11	-24	-13	-16
Karnataka	-9	32	17	-24	-31	-26	-22	-3	-7	-23	-19	-18
Kerala	-1	26	24	-10	-30	-45	-20	-20	-9	-14	-27	-32
Madhya Pradesh	-11	13	5	-13	-16	-14	-4	-13	-7	-9	-14	-10
Maharashtra	-8	-1	-1	-18	11	23	-10	-8	9	-15	3	18
Manipur	45	-37	-37	-4	-26	-24	-20	-5	-6	-7	-21	-19
Meghalaya	-6	3	-8	13	-21	-21	-21	-4	-7	5	-15	-16
Mizoram	31	-16	-22	-15	-20	-22	0	-13	-28	-8	-18	-24
Nagaland	-1	-23	-19	-12	-18	-19	22	-5	-25	0	-13	-18
Odisha	-22	-8	-23	-18	-18	-9	-14	14	12	-18	-5	0
Punjab	-14	9	0	-46	-47	-45	-16	-21	-29	-29	-32	-37
Rajasthan	12	14	-3	-10	-42	-33	-2	-34	-37	-6	-37	-35
Sikkim	-60	-85	-63	-30	16	70	-36	37	-100	-33	15	62
Tamil Nadu	-7	53	49	-18	-40	-40	-23	-6	-22	-20	-23	-32
Telangana	-20	12	-2	-24	4	4	-18	3	5	-21	4	4
Tripura	19	-8	-8	28	-23	-33	-28	-30	-39	8	-27	-32
Uttar Pradesh	18	18	22	-27	-49	-54	-18	-6	-9	-22	-25	-30
Uttarakhand	-15	13	-11	-23	-58	-56	-38	-5	3	-30	-34	-28
West Bengal	-8	17	15	-15	-41	-47	-22	-7	-7	-19	-28	-32
Goa	-40	-5	-23	-30	-28	-16	-26	-3	-18	-29	-18	-16
New Delhi	-2	14	16	-70	-33	-27	-40	9	13	-54	-17	-19

**Table 3: State wise RoC (%) computed during pre-LD, phase-I, phase-II, and total LD for TCN, Terra/MODIS derived AOD<sub>550</sub> and Aqua/MODIS derived AOD<sub>550</sub>.**

## 5 Conclusions

555 The present study was carried out an analysis on air pollution in connection with the world's largest lockdown imposed by the Government of India to contain the spread of COVID-19. The lockdown was extended as 4 lockdowns with strict lockdown from phase-I to several relaxations in phase-IV. However, the lockdown was near-total only in phase-I and II, with the total shutdown of industrial and transport sectors. Thus, we have only considered the first two phases in the present study as total lockdown. We used satellite-based observations of 560 tropospheric TCN, TCC, and AOD<sub>550</sub> pollutant concentrations analysed during the period of lockdown and before LD against the same period of the preceding year (2019) and also against the short-term mean (2014-2019) for about 6 years.

Following are the major findings from the present study

- Due to India's strict LD, the TCN levels are dropped significantly to 18 % across the country compared 565 to the preceding year with a p-value of 0.0007 (confidence interval of 99.93 %).
- Further, analysis is emphasized over the TCN hotspot regions of the Indian sub-continent and observed reduction of (29%) TCN during the total LD period with higher confidence interval.
- The TCN levels with respect to short-term climatological mean are markedly dropped over the urban 570 locations namely New Delhi (- 54%), Bangalore (- 43 %), Chennai (- 41 %), Mumbai (-35 %) and Hyderabad (- 30 %) respectively with high confidence interval about 99.90 %.
- However, during the total LD, an unexpected increase of TCN levels is recorded over the NE region, which is directly correlated with the seasonal biomass burning in this region. This increase is also evaluated statistically against 5-year mean TCN and found insignificant with a p-value of 0.19.
- The TCC levels are decreased during phase-I over IGP, north, and south regions which could be due to 575 the absence of transportation and shutdown of industries. Although variability in the TCC levels was noticed during the total LD period it was tested statistically and found insignificant. Observed high tropospheric CO levels in the NE region during the phase-I LD period, which is mainly attributed to the active fire counts in this region. Also observed low TCC levels in the NE region during phase-II due to the diminished effect of fire counts.
- Since the IGP region is densely populated and clustered industries, which were shut down during phase-I of India's LD, the AOD<sub>550</sub> levels are attained to near baseline in this region (AOD mean value = 0.2). This drastic decrease of AOD<sub>550</sub> in the IGP region was statistically evaluated and found very significant with a p-value of 0.008 with the preceding year (45% decrease) and 50 % reduction against 6-year mean with a p-value <<0.05.

585 • Despite the country's LD, the AOD<sub>550</sub> levels are high over the CI, which was predominantly dominated by the transportation of dust storms and prevailing meteorology. Also observed high AOD<sub>550</sub> over NE and is associated with active fire counts. However, this increase is significant in the CI with a p-value of 0.03 and insignificant in the NE region with a p-value of 0.33, which indicates insignificant change due to LD.

590 • The LD-induced changes in AOD<sub>550</sub> measured by the Terra-Aqua/MODIS show a significant change over the Indian region with very high confidence against the 6-year short-term climatological mean. This variability helps to improve the regional air quality.

• Further, an analysis of RoC was carried out to depict the regional variability of air pollutants during the total LD period in 2020 w.r.t to short-term climatological mean.

595 Therefore, this study successfully demonstrates the satellite-based TCN, TCC, and AOD<sub>550</sub> changes due to India's lockdown during 2020 and compared against the preceding year (2019) and also against the short-term mean picture of 2014-2019.

## 6 Code/Data Availability

600 The satellite and reanalysis data used in the present study are freely available and can be downloaded as summarized in Table 1 with the user's credentials. Python code is uploaded to an online repository ([https://github.com/aarathimuppalla/airpollution\\_ld\\_study.git](https://github.com/aarathimuppalla/airpollution_ld_study.git)) and can be accessed through individual login credentials.

## 605 7 Author Contribution

Conceptualization and Formal analysis are done by MP, AM, SH, DVM, VKS; Writing – original draft, MP, DVM, ALK; Writing – review & editing DVM, ALK, JS, SSR, MVR and UV

## 8 Conflicts of Interest

The authors declare no conflict of interest.

610 **Acknowledgement**

The authors sincerely thank Dr. Raj Kumar, Director NRSC for his support and encouragement in carrying out this study. We greatly acknowledge the Earth data web portal for providing free access to the Aura/OMI, Sentinel-5P/TROPOMI satellites data. We also greatly acknowledge LAADS (Level-1 and Atmosphere Archive and Distribution System) operated by the National Aeronautics and Space Administration (NASA) for providing 615 Aqua-Terra/MODIS satellite data. The authors would also like to thank Land, Atmosphere Near real-time capability for Earth Observation system (LANCE)/ Fire Information for Resource Management System (FIRMS) operated by the NASA for providing the fire data. The authors further thank European Centre for Medium Range Weather Forecasts (ECMWF) for providing the Relative humidity and wind data. We thank Dr. P. Raja, Principal 620 Scientist, Indian Institute of Soil and Water Conservation-Indian Council of Agriculture Research, Ooty, India for reviewing the manuscript. The authors sincerely thank the handling editor and anonymous reviewers for their constructive comments and suggestions for improving the present work.

**References**

625 Alonso, S.M., Deeter, M., Worden, H., Borsdorff, T., Aben, I., Commane, R., Daube, B., Francis, G., George, M., Landgraf, J., Mao, D., McKain, K., and Wofsy, S. : 1.5 years of TROPOMI CO measurements: comparisons to MOPITT and ATom, *Atmos. Meas. Tech.*, 13, 4841–4864, <https://doi.org/10.5194/amt-13-4841-2020>, 2020.

630 Bauwens, M., Compernolle, S., Stavrakou, T., Müller, J. F., Van Gent, J., Eskes, H., Levelt, P.F, Van der A, R., Vreefkind, J. P., Vlietinck, J., Yu, H and Zehner, C.: Impact of Coronavirus Outbreak on NO<sub>2</sub> pollution Assessed Using TROPOMI and OMI observations, *Geophys. Res. Lett.*, 47(11), e2020GL087978, <https://doi.org/10.1029/2020GL087978>, 2020.

635 Beig, G., Korhale, N., Rathod, A., Maji, S., Sahu, S. K., Dole, S., Latha, R., and Murthy, B. S.: On modelling growing menace of household emissions Under COVID-19 in Indian Metros, *Environ. Pollut.*, 272, 115993, <https://doi.org/10.1016/j.envpol.2020.115993>, 2021.

Berman, J. D., and Ebisu, K.: Changes in US air pollution during the COVID-19 pandemic, *Sci. Total Environ.*, 739, 139864, <https://doi.org/10.1016/j.scitotenv.2020.139864>, 2020.

640 Biswal, A., Singh, T., Singh, V., Ravindra, K., and Mor, S. : COVID-19 lockdown and its impact on tropospheric NO<sub>2</sub> concentrations over India using satellite-based data, *Heliyon*, 6(9), e04764. <https://doi.org/10.1016/j.heliyon.2020.e04764>, 2020.

645 Biswal, A., Singh, V., Singh, S., Kesarkar, A. P., Ravindra, K., Sokhi, R. S., Chipperfield, M. P., Dhomse, S. S., Pope, R. J., Singh, T., and Mor, S.: COVID-19 lockdown-induced changes in NO<sub>2</sub> levels across India observed

by multi-satellite and surface observations, *Atmos. Chem. Phys.*, 21, 5235–5251, <https://doi.org/10.5194/acp-21-5235-2021>, 2021.

650 Boucher, O., Randall, D., Artaxo, P., Bretherton, C., Feingold, G., Forster, P., and Rasch, P.: Clouds and aerosols.

Climate change 2013: The physical science basis. Contribution of working group I to the fifth assessment report of the intergovernmental panel on climate change. K., Tignor, M.; Allen, SK, Boschung, J., Nauels, A.; Xia, Y.; Bex, V.; and Midgley, PM, cambridge University Press, Cambridge, UK and New York, NY, USA, <https://www.ipcc.ch/report/ar5/>(last accessed : 5<sup>th</sup> October 2017), 2013.

655 Chance, K., Kurosu, T.P., and Rothman, LS.: OMI Algorithm Theoretical Basis Document Volume IV OMI Trace Gas Algorithms. ATBD-OMI-02, Version 2.0, August 2002.

660 Collivignarelli, M. C., Abbà, A., Bertanza, G., Pedrazzani, R., Ricciardi, P., and Miño, M. C.: Lockdown for CoViD-2019 in Milan: What are the effects on air quality? *Sci. Total Environ.*, 732, 139280, <https://doi.org/10.1016/j.scitotenv.2020.139280>, 2020.

665 David, L.M., Ravishankara, A.R., Kodros, J.K., Venkataraman, C., Sadavarte, P., Pierce, J.R., Chaliyakunnel S., and Millet, D.B.: Aerosol optical depth over India, *J. Geophys. Res. Atmos.*, 123(7), 3688–3703, <https://doi.org/10.1002/2017JD027719>, 2018.

670 Drummond, J. R., and Mand, G. S.: The Measurements of Pollution in the Troposphere (MOPITT) instrument: Overall performance and calibration requirements, *J. Atmos. Ocean. Technol.*, 13(2), 314–320, 1996.

Eskes, H., van Geffen, J., Boersma, F., Eichmann, K.-U., Apituley, A., Pedergnana, M., Sneep, M., Veefkind, J. P., and Loyola, D.: Sentinel-5 precursor/TROPOMI Level 2 Product User Manual Nitrogendioxide, Tech. Rep. S5P-KNMI-L2- 0021-MA, Koninklijk Nederlands Meteorologisch Instituut (KNMI), available at: <https://sentinel.esa.int/documents/247904/2474726/Sentinel-5P-Level-2-Product-User-Manual-Nitrogen-Dioxide> (last access: 15<sup>th</sup> January 2021), CI-7570-PUM, issue 3.0.0, 2019.

675 Fang, M., Chan, C.K., and Yao, X.: Managing air quality in a rapidly developing nation: China, *Atmos. Environ.*, 43, 79–86, doi:10.1016/j.atmosenv.2008.09.064, 2009.

Freedman, D. A., Pisani, R. and Purves, R. Statistics 93–110 (W. W. Norton & Co Inc, New York, 2007).

680 Garg, A., Kapshe, M., Shukla, P. R., and Ghosh, D.: Large point source (LPS) emissions from India: regional and sectoral analysis, *Atmos. Environ.*, 36(2), 213–224, [https://doi.org/10.1016/S1352-2310\(01\)00439-3](https://doi.org/10.1016/S1352-2310(01)00439-3), 2002.

685 Ghude, S. D., Fadnavis, S., Beig, G., Polade, S. D., and Van Der A, R. J. : Detection of surface emission hot spots, trends, and seasonal cycle from satellite retrieved NO<sub>2</sub> over India, *J. Geophys. Res. Atmos.*, 113(D20), <https://doi.org/10.1029/2007JD009615>, 2008.

690 Hubanks, P., Platnick, S., King, M., and Ridgway, B.: MODIS Algorithm Theoretical Basis Document No: ATBD-MOD-30 for Level-3 Global Gridded Atmosphere Products (08\_D3, 08\_E3, 08\_M3) and Users Guide. Collection 6.1, Version 4.5, 6<sup>th</sup> August 2020.

Hsu, N. C., Lee, J., Sayer, A. M., Kim, W., Bettenhausen, C., and Tsay, S. C.: VIIRS Deep Blue Aerosol Products Over Land: Extending the EOS long- Term Aerosol Data Records, *J. Geophys. Res. Atmos.*, 124(7), 4026-4053, <https://doi.org/10.1029/2018JD029688>, 2019.

695 Jephcott, C., Hansell, A. L., Adams, K., and Gulliver, J. : Changes in air quality during COVID-19 'lockdown' in the United Kingdom. *Environ. Pollut.*, 272, 116011. <https://doi.org/10.1016/j.envpol.2020.116011>, 2021.

700 Kanchana, A. L., Sagar, V. K., Pathakoti, M., Mahalakshmi, D. V., Mallikarjun, K., and Gharai, B.: Ozone variability: Influence by its precursors and meteorological parameters-an investigation, *J. Atmos. Sol.-Terr. Phys.*, 211, 105468, <https://doi.org/10.1016/j.jastp.2020.105468>, 2020.

705 Krotkov, N. A., Lamsal, L. N., Celarier, E. A., Swartz, W. H., Marchenko, S. V., Bucsela, E. J., Chan, K.L., Wenig, M., and Zara, M.: The version 3 OMI NO<sub>2</sub> standard product, *Atmos. Meas. Tech.*, 10(9), 3133-3149, <https://doi.org/10.5194/amt-10-3133-2017>, 2017.

710 Lal, Preet., Kumar, A., Kumar, S., Kumari, S., Saikia, P., Dayanandan, A., Adhikari, D., and Khan, M.L.: The dark cloud with a silver lining: Assessing the impact of the SARS COVID-19 pandemic on the global environment, *Sci. Total Environ.* 732, 139297, <https://doi.org/10.1016/j.scitotenv.2020.139297>, 2020.

715 Landgraf, J., Brugh, J.A.D., Scheepmaker, R.A., Borsdoff, T., Houweling, S., and Hasekamp, O.P.: Algorithm Theoretical Baseline Document for Sentinel-5 Precursor: Carbon Monoxide Total Column Retrieval. SRON-S5P-LEV2-RP-002, issue 1.10, 15 June 2018.

720 Levy, R.C., Mattoo, S., Munchak, L.A., Remer, L.A., Sayer, A.M., Patadia, F., and Hsu, N.C.: The Collection 6 MODIS aerosol products over land and ocean, *Atmos. Meas. Tech.* 6, 2989-3034, doi:10.5194/amt-6-2989-2013, 2013.

725 Li, R., Mei, X., Chen, L., Wang, L., Wang, Z., and Jing, Y.: Long-Term (2005–2017) View of Atmospheric Pollutants in Central China Using Multiple Satellite Observations, *Remote Sens.*, 12(6), 1041, <https://doi.org/10.3390/rs12061041>, 2020.

730 Mahalakshmi, D.V., Sujatha, P., Naidu, C.V., and Chowdary, V. M.: Contribution of vehicular emissions on urban air quality: results from public strike in Hyderabad, *Indian J. Radio Space Phys.* 43, 340-348, 2014.

735 Mahalakshmi, D. V., Sujatha, P., Naidu, C. V., and Chowdary, V. M.: Response of vehicular emissions to air pollution and radiation-A case study during public strike in Hyderabad, India, *Sustain. Environ. Res.*, 25(4), 227-234, 2015.

730 Mahato, S., Pal, S., and Ghosh, K. G.: Effect of lockdown amid COVID-19 pandemic on air quality of the megacity Delhi, India, *Sci. Total Environ.*, 730, <https://doi.org/10.1016/j.scitotenv.2020.139086>, 2020.

735 Mor, S., Kumar, S., Singh, T., Dogra, S., Pandey, V., and Ravindra, K. : Impact of COVID-19 lockdown on air quality in Chandigarh, India: Understanding the emission sources during controlled anthropogenic activities. *Chemosphere*, 127978, <https://doi.org/10.1016/j.chemosphere.2020.127978> , 2020.

Nishanth, T., Praseed, K., Kumar, M.K.S., and Valsaraj, K.T.: Observational study of surface O<sub>3</sub>, NO<sub>x</sub>, CH<sub>4</sub> and total NMHCs at Kannur, India, *Aerosol Air Qual. Res.*, 14(3), 1074-1088, doi: 10.4209/aaqr.2012.11.0323, 2014.

740 Pandey, S.K., and Vinoj, V.: Surprising Changes in Aerosol Loading over India amid COVID-19 Lockdown, *Aerosol Air Qual. Res.* 21, 200466, <https://doi.org/10.4209/aaqr.2020.07.0466>, 2020.

Ramachandran, S., and Kedia, S: Aerosol-precipitation interactions over India: review and future perspectives, *Adv Meteorol*, <https://doi.org/10.1155/2013/649156>., 2013.

745 Ramachandran, A., Jain, N. K., Sharma, S. A., and Pallipad, J.: Recent trends in tropospheric NO<sub>2</sub> over India observed by SCIAMACHY: Identification of hot spots, *Atmospheric Pollut. Res.*, 4(4), 354-361. <https://doi.org/10.5094/APR.2013.040>, 2013.

750 Ranjan, AK, Patra, AK, and Gorai, AK.: Effect of lockdown due to SARS COVID-19 on aerosol optical depth (AOD) over urban and mining regions in India, *Sci. Total Environ.*, 745, 141024. [10.1016/j.scitotenv.2020.141024](https://doi.org/10.1016/j.scitotenv.2020.141024), 2020.

Ratnam, V., Prasad, P., Raj, S. A., and Ibrahim, H.: Effect of Lockdown due to COVID-19 on the Aerosol and Trace Gases Spatial Distribution over India and Adjoining Regions, *Aerosol Air Qual. Res.*, 20, <https://doi.org/10.4209/aaqr.2020.07.0397>.

755 Sayer, A. M., Hsu, N. C., Bettenhausen, C., and Jeong, M. J.: Validation and uncertainty estimates for MODIS Collection 6 “Deep Blue” aerosol data, *J. Geophys. Res. Atmos.*, 118(14), 7864-7872, <https://doi.org/10.1002/jgrd.50600>, 2013.

760 Sayer, A. M., Hsu, N. C., Lee, J., Kim, W. V., and Dutcher, S. T.: Validation, stability, and consistency of MODIS Collection 6.1 and VIIRS Version 1 Deep Blue aerosol data over land, *J. Geophys. Res. Atmos.*, 124(8), 4658-4688, <https://doi.org/10.1029/2018JD029598>, 2019.

765 Singh, R.P., and Chauhan, A.: Impact of lockdown on air quality in India during COVID-19 pandemic, *Air Qual Atmos Health* 13, 921-928, <https://doi.org/10.1007/s11869-020-00863-1>, 2020.

770 Tian, H., Liu, Y., Li, Y., Wu, C., Chen, B., Kraemer, M., Li, B., Cai, J., Xu, B., Yang, Q., Wang, B., Yang, P., Cui, Y., Song, Y., Zheng, P., Wang, Q., Bjornstad, O., Yang, R., Grenfell, B., Pybus, O., and Dye, C.: An investigation of transmission control measures during the first 50 days of the COVID-19 epidemic in China, *Science*, 368, 638-642, doi: 10.1126/science.abb6105, 2020.

Van Geffen, J., Eskes, H. J., Boersma, K. F., Maasakkers, J. D. , and Veefkind, J. P. : TROPOMI ATBD of the total and tropospheric NO<sub>2</sub> data products. Royal Netherlands Meteorological Institute, S5P-KNMI-L2-0005-RP, issue 1.4.0, 2019.

775 Verma, M., Pervez, S., Deb, M. K., and Majumdar, D.: Domestic use of cooking fuel in India: A Review on Emission Characteristics and Associated Health Concerns, *Asian J Chem*, 30(2), 235-245, <https://doi.org/10.14233/ajchem.2018.21006>, 2018.

780 World Health Organization (WHO): Review of evidence on health aspects of air pollution—REVIHAAP project: final technical report. Bonn: WHO European Centre for Environment and Health, 2013.

Xu, K., Cui, K., Young, L., Hsieh, Y., Wang, Y., Zhang, J., and Wan, S.: Impact of the COVID-19 Event on Air Quality in Central China, *Aerosol Air Qual Res.*, 20(5), 915-929, doi: 10.4209/aaqr.2020.04.0150, 2020.